J. Fluid Mech. (1982), *vol.* 121, *pp.* 187–206
Printed in Great Britain

The instability of sheared liquid layers

By MARC K. SMITH AND STEPHEN H. DAVIS

Department of Engineering Sciences and Applied Mathematics,
The Technological Institute, Northwestern University,
Evanston, Illinois 60201, U.S.A.

(Received 3 September 1981)

A prescribed shear stress applied to the free surface of a thin liquid layer sets up a steady shear flow. When the shear flow has a linear velocity profile, Miles, using asymptotic analysis, finds critical values R_c of the Reynolds number above which unstable travelling waves exist. However, Miles omits a term in the normal-stress boundary condition. We correct this omission and solve the appropriate Orr–Sommerfeld system numerically to obtain the critical conditions. For the case of a zero-surface-tension interface, we find that $R_c = 34{\cdot}2$, as compared with Miles' value of $R_c = 203$. As surface tension increases, R_c asymptotes to the inviscid limit developed by Miles. The critical Reynolds number, critical wavenumber and critical phase speed are presented as functions of a non-dimensional surface tension. We investigate the mechanism of the instability through an examination of the disturbance-energy equation. When the shear flow has a parabolic velocity profile, we find a long-wave instability at small values of the Reynolds number. Numerical methods are used to extend these results to larger values of the wavenumber. Examination is made of the relation between this long-wave instability and profile curvature.

1. Introduction

Consider a liquid layer of infinite horizontal extent bounded below by a rigid plane and above by a free surface. If a prescribed shear stress is applied to the free surface, then unstable travelling surface waves may exist. These surface waves are driven by the bulk flow, having a linear velocity profile, and by the work done during deformation by the applied shear stress on the free surface.

Miles (1960) discusses this model as appropriate to nosecone ablation and film cooling if 'the only significant role of the much lighter fluid flowing over the film is to produce the mean shear flow'. He then poses a boundary-value problem and uses linear theory to investigate its stability characteristics. However, the problem he poses is actually a special limit of the two-fluid model proposed by Feldman (1957), in which the upper fluid has small density and viscosity but large kinematic viscosity. Miles errs in assuming equivalence between this limiting case of the two-layer model and the single layer with applied shear, the latter having an extra term in the normal-stress boundary condition.

Our interest in this model arises from the study of a shear flow in a liquid film driven by surface-tension gradients along the free surface. In certain parametric limits of this thermocapillary flow (Smith & Davis 1981), the stability characteristics of this non-

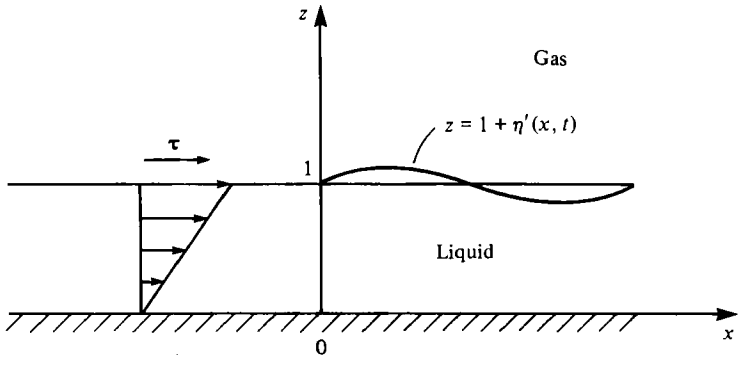

FIGURE 1. A sketch of the geometry of the liquid layer with the basic-state velocity profile and surface disturbances indicated.

isothermal system are determined by the stability of the isothermal film flow described above. Hence a full understanding of the isothermal problem is desirable.

Rather than following Miles and using an asymptotic theory for large Reynolds numbers, we solve the appropriate Orr–Sommerfeld system for this problem numerically and find the critical Reynolds number R_c. Here R is a non-dimensional prescribed shear stress based on the mean depth of the layer. For zero surface tension the Miles asymptotics yields $R_c = 203$, while our numerical solution of Miles' equations yields $R_c = 78{\cdot}6$. The numerical solution of the corrected Orr–Sommerfeld system for this model yields $R_c = 34{\cdot}2$. We obtain R_c for a wide range of surface tensions and discuss in detail the stability characteristics of this flow.

When a viscous liquid fills a two-dimensional slot (having end walls), an imposed shear stress on its free surface induces a complicated recirculating flow. Sen & Davis (1982) have obtained one such steady flow for thin slots when the motion is induced by thermocapillarity. Similar methods show for the present case with large surface tension that an approximately parallel flow can exist in the core (away from the end walls). Here the free surface is approximately flat and the velocity profile is parabolic. We investigate the stability of this core flow and find a long-wave instability at small values of the Reynolds number. We obtain the stability characteristics for a wide range of wavenumbers by solving numerically the appropriate Orr–Sommerfeld system.

The appearance of a long-wave instability for the parabolic velocity profile but not for the linear velocity profile leads us to investigate the conditions under which such long waves are possible. We relate their appearance to profile curvature and bulk pressure gradients.

Finally, we discuss relevant experiments on sheared liquid layers in terms of the present results.

2. Formulation

2.1. *The mathematical model*

Consider a liquid layer of infinite horizontal extent bounded by a rigid plane at $z = 0$ and a free surface having mean position at $z = d$. The layer, shown in figure 1, is composed of an incompressible Newtonian liquid with constant viscosity μ, density ρ,

and surface tension σ. A constant shear stress of magnitude τ is applied at the free surface. There are no body forces.

The origin of the Cartesian co-ordinate system lies on the rigid plane, and all distances in this system are scaled on the liquid depth d. The system is assumed two-dimensional, so that all variables are independent of y. The velocity vector $\mathbf{v} = (u, w)$, pressure p and time t are referred to scales $\tau d/\mu, \tau$ and μ/τ respectively. As a result, there arise the following non-dimensional groups:

$$R \equiv \rho d^2 \tau/\mu^2, \quad S \equiv \rho d\sigma/\mu^2. \tag{2.1a,b}$$

R is the Reynolds number and S is a non-dimensional surface tension.

In general, the free surface is located at $z = 1+\eta(x,t)$, where the mean value of $\eta(x,t)$ is zero. Thus, we define the unit normal and tangential vectors to the free surface as follows:

$$\mathbf{n} = (-\eta_x, 1)/N, \quad \mathbf{t} = (1, \eta_x)/N, \tag{2.2a,b}$$

where

$$N = (1+\eta_x^2)^{\frac{1}{2}}, \tag{2.2c}$$

and subscripts denote partial differentiation. On the free surface the normal stress balances the surface tension times the curvature and the shear stress is prescribed. This can be expressed through the following vector equation:

$$\sigma_{ij} n_j = SR^{-1} K(\eta)\, n_i + t_i \quad \text{on} \quad z = 1+\eta. \tag{2.3a}$$

Here σ_{ij} is the stress tensor of the liquid,

$$\sigma_{ij} = -p\delta_{ij} + \epsilon_{ij}, \tag{2.3b}$$

where

$$\epsilon_{ij} = v_{i,j} + v_{j,i}, \tag{2.3c}$$

and $K(\eta)$ is the curvature of the free surface,

$$K(\eta) = \eta_{xx}/N^3. \tag{2.3d}$$

Commas denote spatial differentiation, δ_{ij} is the Kronecker delta, and the summation convention is used over the range $i = 1, 3$. The bounding gas is passive with a constant pressure taken equal to zero. The kinematic condition on the free surface is written as

$$w = \eta_t + u\eta_x \quad \text{on} \quad z = 1+\eta. \tag{2.4}$$

On the rigid plane there is no slip,

$$v_i = 0 \quad \text{on} \quad z = 0. \tag{2.5}$$

The governing bulk equations for the liquid layer are the Navier–Stokes and continuity equations

$$R\left(\frac{\partial v_i}{\partial t} + v_j v_{i,j}\right) = -p_{,i} + \nabla^2 v_i, \tag{2.6a}$$

$$v_{i,i} = 0. \tag{2.6b}$$

2.2. *The basic state*

Consistent with the system defined by (2.2)–(2.6) we find the following basic-state solution:

$$\bar{\mathbf{v}} = (\bar{u}, \bar{w}) = (z, 0), \tag{2.7a}$$

$$\bar{p} = 0, \quad \bar{\eta} = 0, \tag{2.7b,c}$$

with the unit normal and tangential vectors to the free surface given as

$$\mathbf{N} = (0, 1) \equiv \mathbf{n}|_{\eta_x=0}, \tag{2.7d}$$

$$\mathbf{T} = (1, 0) \equiv \mathbf{t}|_{\eta_x=0}. \tag{2.7e}$$

2.3. *The linearized stability analysis*

In a standard way, we apply infinitesimal two-dimensional disturbances to the system as follows:

$$\mathbf{v} = \bar{\mathbf{v}} + \mathbf{v}'(x, z, t), \tag{2.8a}$$

$$p = \bar{p} + p'(x, z, t), \tag{2.8b}$$

where the free surface is located at

$$z = 1 + \eta'(x, t). \tag{2.8c}$$

These are substituted into the governing equations and boundary conditions, and we then linearize in the disturbance quantities. It is sufficient to consider only two-dimensional disturbances because it is possible to prove Squire's theorem for this problem.

The linearized system governing two-dimensional disturbances of infinitesimal amplitude is as follows:

$$R\left(\frac{\partial v_i'}{\partial t} + \bar{u}\frac{\partial v_i'}{\partial x} + \frac{d\bar{u}}{dz}w'T_i\right) = -p'_{,i} + \nabla^2 v_i', \tag{2.9a}$$

$$v'_{i,i} = 0, \tag{2.9b}$$

$$v_i' = 0 \quad \text{on} \quad z = 0, \tag{2.9c}$$

$$w' = \eta_t' + \bar{u}\eta_x' \quad \text{on} \quad z = 1, \tag{2.9d}$$

$$\sigma'_{ij}N_j = \left\{SR^{-1}\eta'_{xx} + 2\frac{d\bar{u}}{dz}(1)\eta_x'\right\}N_i - \frac{d^2\bar{u}}{dz^2}(1)\eta' T_i \quad \text{on} \quad z = 1. \tag{2.9e}$$

We introduce a disturbance stream function ψ,

$$u' = \psi_z, \quad w' = -\psi_x, \tag{2.10}$$

and normal modes as follows:

$$(\psi(x, z, t), p'(x, z, t), \eta'(x, t)) = (\phi(z), P(z), \hat{\eta})\exp[i\alpha(x - ct)], \tag{2.11}$$

where $\alpha > 0$. The complex eigenvalue

$$c = c_R + ic_I \tag{2.12}$$

consists of the phase speed c_R and the growth rate αc_I of the disturbances. The forms (2.10) and (2.11) are substituted into the system (2.9), where cross differentiation is used to eliminate $P(z)$ and the kinematic condition (2.9d) is used to eliminate $\hat{\eta}$. The following Orr–Sommerfeld system is obtained:

$$(D^2 - \alpha^2)^2\phi = i\alpha R[(\bar{u} - c)(D^2 - \alpha^2)\phi - \bar{u}''\phi], \tag{2.13a}$$

$$\phi(0) = \phi'(0) = 0, \tag{2.13b, c}$$

$$\phi''(1) + \left\{-\frac{\bar{u}''(1)}{[\bar{u}(1) - c]} + \alpha^2\right\}\phi(1) = 0, \tag{2.13d}$$

$$\phi'''(1) - \{i\alpha R[\bar{u}(1) - c] + 3\alpha^2\}\phi'(1) + \left\{i\alpha R\bar{u}'(1) + \frac{2\bar{u}'(1)\alpha^2}{[\bar{u}(1) - c]} + \frac{iS\alpha^3}{R[\bar{u}(1) - c]}\right\}\phi(1) = 0, \tag{2.13e}$$

where $D \equiv d/dz$ and primes on $\bar{u}$ denote d/dz. For the basic state under consideration $\bar{u}(z) = z$.

The formulation of the Orr–Sommerfeld system in Miles (1960) omits the term $2(d\bar{u}/dz)(1)\eta_x'$ in the normal-stress boundary condition (2.9*e*), which corresponds to the term $2\bar{u}'(1)\alpha^2\phi(1)/[\bar{u}(1)-c]$ in (2.13*e*). Otherwise, his system is identical to system (2.13). This omitted term arises from disturbances of the unit normal and tangent vectors at the free surface which result in contributions to the normal-stress perturbation through the basic-state shear stress applied at the interface.

3. The inviscid problem

Following Miles (1960), we define a reciprocal Weber number

$$T \equiv S/R^2, \tag{3.1}$$

and examine the limit of system (2.13) as $R \to \infty$ with T fixed. Using the basic-state velocity $\bar{u}(z) = z$, we obtain the following inviscid stability problem:

$$\phi'' - \alpha^2\phi = 0, \quad \phi(0) = 0, \tag{3.2a, b}$$

$$(1-c)\,\phi'(1) - \phi(1) - \frac{T\alpha^2}{(1-c)}\phi(1) = 0. \tag{3.2c}$$

The characteristic equation associated with the system (3.2) is

$$1 - c = \frac{\tanh\alpha}{2\alpha}\left[1 \pm \left(1 + \frac{4\alpha^3 T}{\tanh\alpha}\right)^{\frac{1}{2}}\right]. \tag{3.3}$$

This result is *identical* with that obtained by Miles (1960) since the omitted term in condition (2.13*e*) vanishes as $R \to \infty$.

If instead of T we had fixed the surface tension number S as $R \to \infty$, then we would have found that

$$1 - c = \frac{\tanh\alpha}{\alpha}. \tag{3.4}$$

As can be seen from the forms (3.3) and (3.4), the eigenvalue c is real, indicating that the growth rates of the disturbances are zero. Thus, a liquid layer set into motion by an applied shear stress on its free surface is *inviscidly stable*.

It can be shown in the same manner as Howard (1961) that for inviscidly unstable modes, i.e. $c_I > 0$,

$$0 < c_R < 1. \tag{3.5}$$

For the eigenvalue c defined in the form (3.3) to be a valid approximation of the eigenvalue of the system (2.13) as $R \to \infty$, it must also satisfy the inequality (3.5).

Using $c < 1$, we can discard the minus sign in the form (3.3). Using $c > 0$, we find that the form (3.3) leads to the result

$$T < f(\alpha) \equiv \alpha^{-1}\coth\alpha - \alpha^{-2}. \tag{3.6}$$

The function $f(\alpha)$ is a monotonically decreasing function of α with a maximum at $\alpha = 0$ of $f(0) = \frac{1}{3}$. If the inequality (3.6) is violated, then the eigenvalue does not lie in the interval (0, 1) and no unstable mode exists. Thus we regain Miles' (1960) result that a sufficient condition for stability as $R \to \infty$ is

$$T \geqslant \tfrac{1}{3}. \tag{3.7a}$$

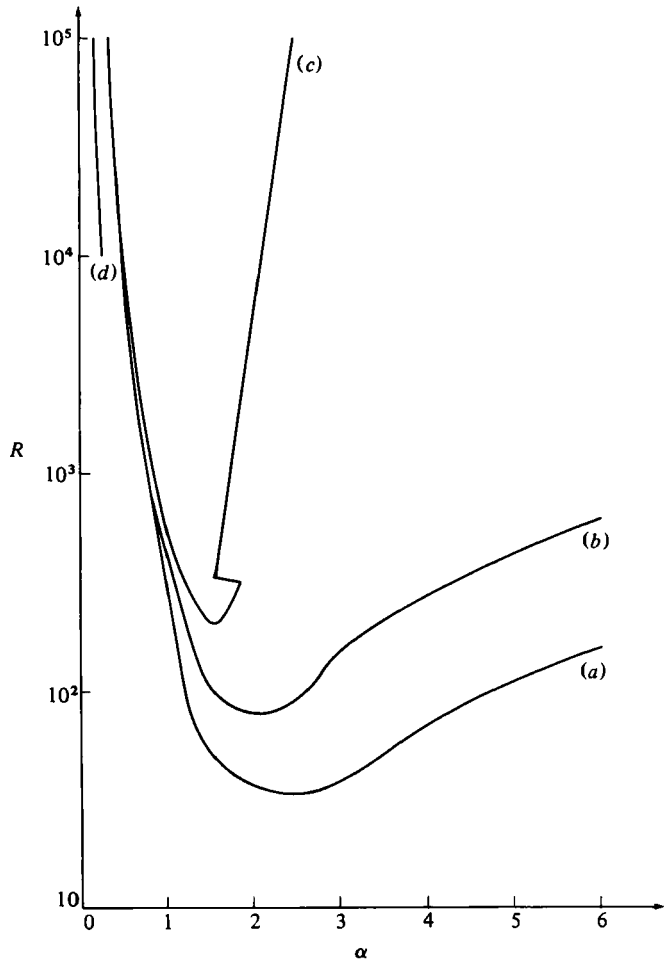

FIGURE 2. A comparison of three neutral stability curves for the linear velocity profile $\bar{u}$ for $S = 0$: (*a*) the curve obtained by numerical integration of the Orr–Sommerfeld system (2.13); (*b*) the curve obtained by numerical integration of the Orr–Sommerfeld system used by Miles (1960); (*c*) the curve obtained by Miles (1960) using an asymptotic analysis. Curve (*d*) is $R = \alpha^{-7}$. The curves (*a*)–(*c*) have the asymptotic behaviour $R \sim \alpha^{-7}$ as $\alpha \to 0$.

In our notation, this gives the large-Reynolds-number asymptote for stability,

$$R \leqslant (3S)^{\frac{1}{2}}. \tag{3.7b}$$

4. Method of solution for finite R

We solve the eigenvalue problem (2.13) numerically using a computer code called SUPORT written by Scott & Watts (1975, 1977). This code employs a shooting method, and during the integration process uses orthonormalization to maintain a linearly independent set of solution vectors. In addition, the secant method is used to converge on system eigenvalues.

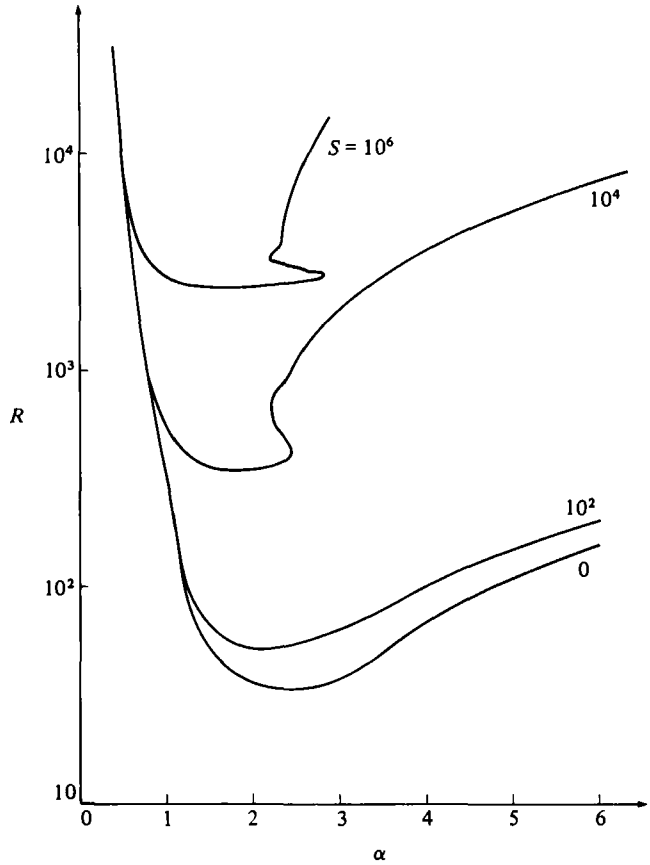

FIGURE 3. Neutral stability curves for the linear velocity profile $\bar{u}$ for various values of S. All curves have the asymptotic behaviour $R \sim \alpha^{-7}$ as $\alpha \to 0$.

5. Results

In figure 2, three neutral curves with $S = 0$ are compared. The lowest curve represents the numerical result for the system (2.13), and has a minimum of $R = R_c = 34{\cdot}2$ at $\alpha = \alpha_c = 2{\cdot}43$. The middle curve represents our numerical result for the eigenvalue system as formulated by Miles (1960), and has a minimum of $R = R_c = 78{\cdot}6$ at $\alpha = \alpha_c = 2{\cdot}1$. Thus we see that the omitted term in the normal-stress boundary condition causes an overestimate of R_c by about a factor of two. The third curve in figure 2 is our redrawing of the $S = 0$ (i.e. $T = 0$) curve obtained by Miles (1960) and shown in figure 4(*a*) of his paper. This curve was computed using an asymptotic theory, and has a minimum of $R = R_c = 203$ at $\alpha = \alpha_c = 1{\cdot}6$. The difference between the critical Reynolds number of 78·6 found by a numerical technique and the value of 203 found using asymptotic theory can be accounted for by noting that the asymptotic theory is valid for $(\alpha R)^{\frac{1}{3}} \gg 1$ and also that the approximation (3.8) of Miles (1960) is valid for $(\alpha R)^{\frac{2}{3}} \gg \alpha^2$. Both of these conditions are only barely satisfied for $R = 78{\cdot}6$ and $\alpha = 2{\cdot}1$. However, as $\alpha \to 0$ all three curves have the *same* asymptote $R \sim \alpha^{-7}$, as derived by Miles (1960). In this limit, the asymptotic approximation becomes more accurate and the omitted term in the normal-stress boundary condition, being $O(\alpha^2)$,

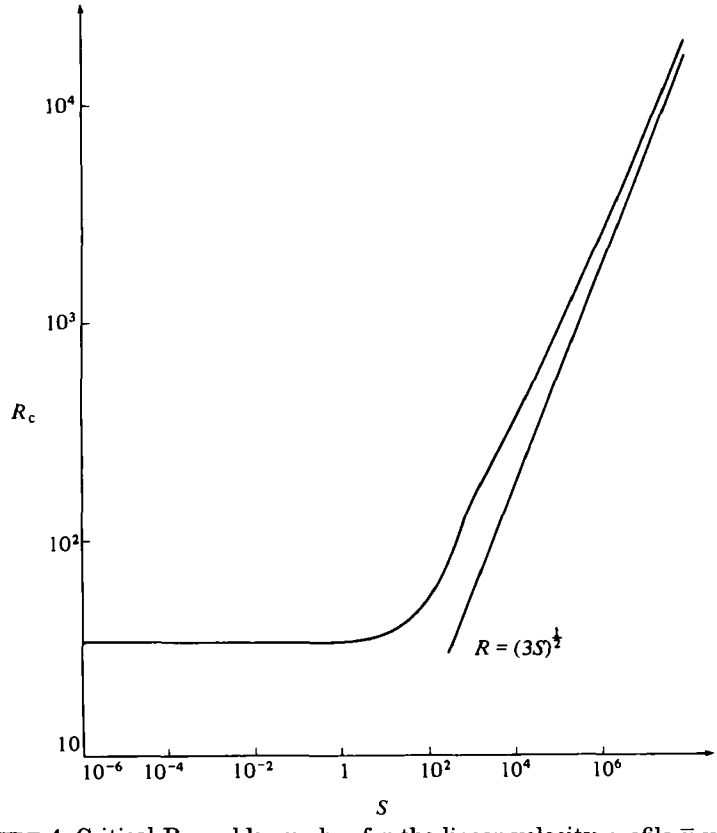

FIGURE 4. Critical Reynolds number for the linear velocity profile $\bar{u}$ versus S. The inviscid limit is the line $R = (3S)^{\frac{1}{2}}$.

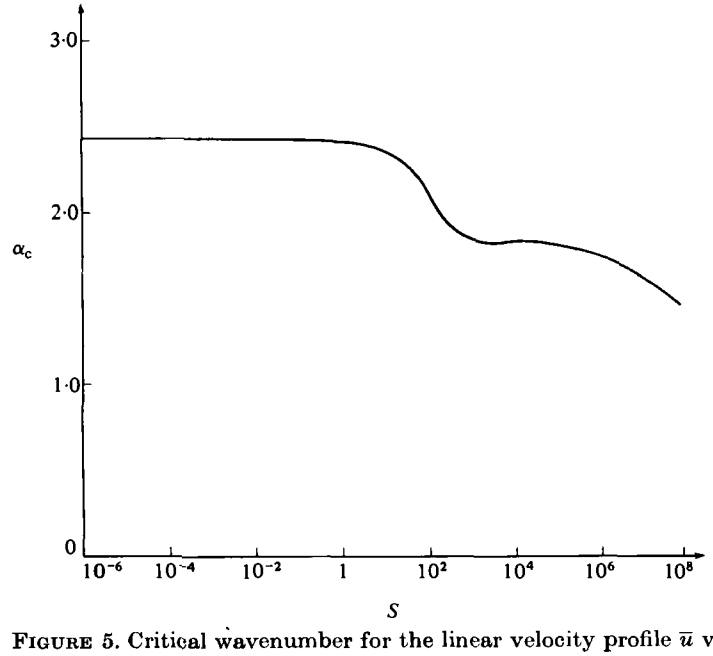

FIGURE 5. Critical wavenumber for the linear velocity profile $\bar{u}$ versus S.

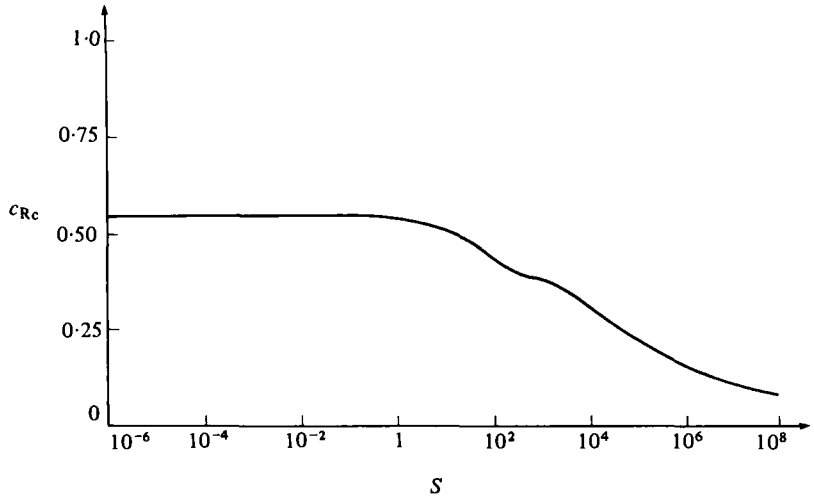

FIGURE 6. Critical phase speed for the linear velocity profile $\bar{u}$ versus S.

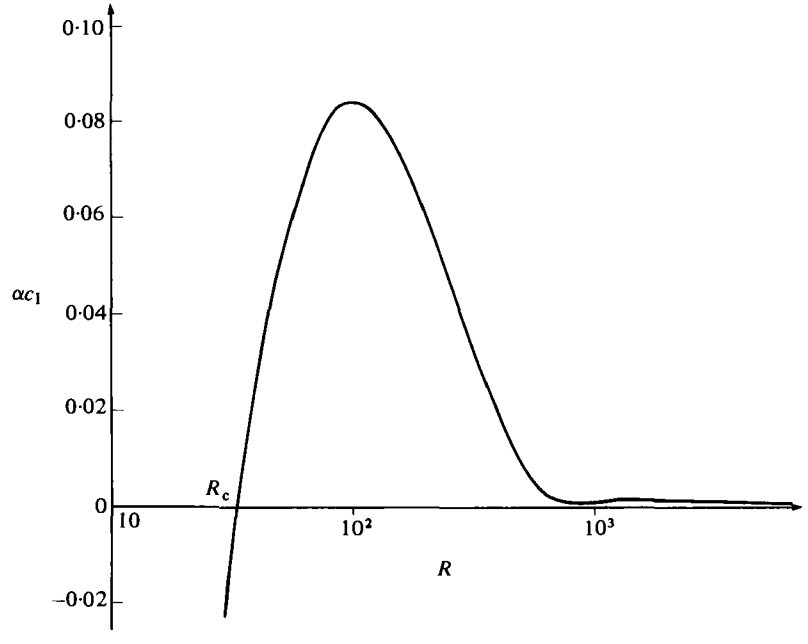

FIGURE 7. The disturbance growth rate for the linear velocity profile $\bar{u}$ versus Reynolds number for fixed $S = 0$ and $\alpha = \alpha_c = 2{\cdot}43$. The maximum of $\alpha c_I = 0{\cdot}08411$ occurs at $R = 100$.

is negligible compared with the $O(\alpha)$ terms. Note that the case illustrated, $S = 0$, is a worst case for Miles' results. As S increases, so does R_c, and the omitted term becomes relatively smaller while the asymptotics become more accurate.

The eigenvalue problem (2.13) was solved for S between zero and 10^8. Neutral curves for four values in this range are shown in figure 3. Again, all these curves have the form $R > \alpha^{-7}$ as $\alpha \to 0$.

Figure 4 shows the stabilizing effect of surface tension in that R_c increases with S. This curve asymptotes to the line $R = (3S)^{\frac{1}{2}}$ for large S, since as S increases R_c becomes

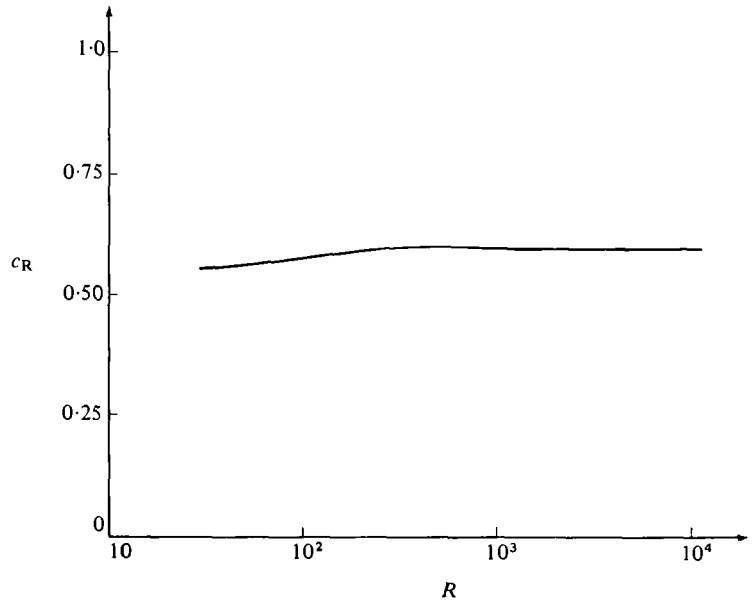

FIGURE 8. The corresponding phase speed for the linear velocity profile $\bar{u}$ versus Reynolds number for fixed $S = 0$ and $\alpha = \alpha_c = 2{\cdot}43$. As $R \to \infty$, $c_R \to 0{\cdot}5948$.

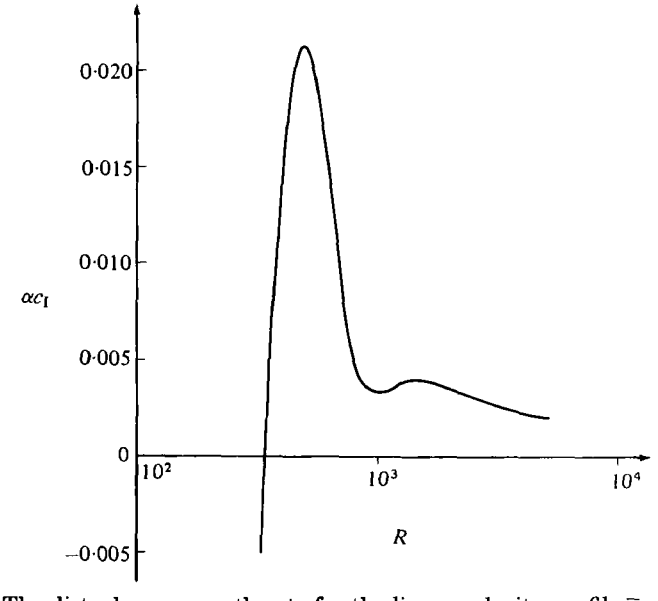

FIGURE 9. The disturbance growth rate for the linear velocity profile $\bar{u}$ versus Reynolds number for fixed $S = 10^4$ and $\alpha = \alpha_c = 1{\cdot}85$. The maximum of $\alpha c_I = 0{\cdot}021\,33$ occurs at $R = 501$.

large and the inviscid limit (3.7) is approached. Each point on this curve corresponds to a different value of α_c because α_c depends on S as shown in figure 5. As S increases, the surface becomes 'stiffer' and therefore more resistive to short-wavelength corrugations. This accounts for the generally decreasing behaviour of α_c with increasing S.

Figure 6 shows that the critical phase speed c_{Rc} decreases with increasing S. As

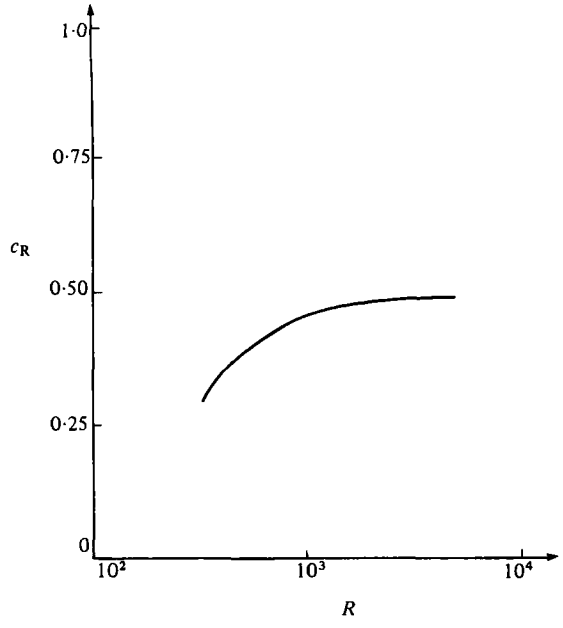

FIGURE 10. The corresponding phase speed for the linear velocity profile $\bar{u}$ versus Reynolds number for fixed $S = 10^4$ and $\alpha = \alpha_c = 1{\cdot}85$. As $R \to \infty$, $c_R \to 0{\cdot}4855$.

before, for large S the inviscid limit is approached and the decreasing behaviours of α_c and c_{Rc} with increasing S are connected through the inviscid relation (3.3).

Often in free-surface problems the application of linear stability theory to experimental observation becomes difficult because the growth rates of the disturbances are so small that the disturbances cannot be sensed until R exceeds R_c by an appreciable amount. Hence it is of some interest to have estimates of the growth rates for $R > R_c$.

In our estimates, we fix S and $\alpha = \alpha_c$ and allow R to increase through R_c. Note that $\alpha = \alpha_c$ does *not* necessarily correspond to the wavenumber with maximum growth rate for $R > R_c$, even though it does have this property for $R = R_c$. Figure 7 shows αc_I versus R for $S = 0$ and $\alpha = \alpha_c = 2{\cdot}43$. For $R < R_c$, $\alpha c_I < 0$, then it increases with R, vanishes at R_c, increases to a maximum of $\alpha c_I = 0{\cdot}084\,11$ at $R = 100$, and then decreases to zero as $R \to \infty$. This decrease is consistent with the fact that the shear flow is inviscidly stable. Figure 8 gives the corresponding values of the phase speed c_R as R is increased. Here we note that the limiting value of c_R as $R \to \infty$ is given by (3.4). Figures 9 and 10 give curves of αc_I and c_R versus R for $S = 10^4$ and $\alpha = \alpha_c = 1{\cdot}85$. Here, the maximum growth rate is $\alpha c_I = 0{\cdot}021\,33$ at $R = 501$.

6. Energetics

The mechanism of instability can be investigated by evaluating the mechanical-energy balance for this system. Furthermore, this computation is an independent check on the numerical consistency of the linear stability analysis. The energy-balance equation is obtained by multiplying the linear disturbance equation (2.9*a*) by v_i', integrating over the volume $\mathscr{V}$: $0 \leqslant x \leqslant 2\pi/\alpha$, $0 \leqslant z \leqslant 1$, and then using Green's theorem and the continuity equation (2.9*b*). The result is

$$\frac{d\mathscr{E}}{dt} = \mathscr{P} + R^{-1}\mathscr{S} - R^{-1}\mathscr{D}, \tag{6.1a}$$

where

$$\mathscr{E} = \frac{1}{2}\int_{\mathscr{V}} (v_i'^2) \tag{6.1b}$$

is the disturbance kinetic energy,

$$\mathscr{P} = \int_{\mathscr{V}} \left(-\frac{d\overline{u}}{dz} u'w'\right) \tag{6.1c}$$

is the disturbance-energy production due to Reynolds stresses,

$$\mathscr{S} = \int_0^{2\pi/\alpha} [\sigma'_{ij} N_j v'_i]_{z=1}\, dx \tag{6.1d}$$

is the disturbance-energy production due to surface-stress working, and

$$\mathscr{D} = \int_{\mathscr{V}} (\tfrac{1}{2} e'^2_{ij}) \tag{6.1e}$$

is the disturbance viscous dissipation. Using the boundary condition (2.9e), $\mathscr{S}$ can be transformed into the equivalent form

$$\mathscr{S} = \mathscr{S}_{\mathrm{ST}} + \mathscr{S}_{\mathrm{NBS}} + \mathscr{S}_{\mathrm{TS}}, \tag{6.2a}$$

where

$$\mathscr{S}_{\mathrm{ST}} = \int_0^{2\pi/\alpha} [SR^{-1}\eta'_{xx} w']_{z=1}\, dx, \tag{6.2b}$$

is the work done by surface-tension forces,

$$\mathscr{S}_{\mathrm{NBS}} = \int_0^{2\pi/\alpha} \left[2\frac{d\overline{u}}{dz}(1)\,\eta'_x w'\right]_{z=1} dx, \tag{6.2c}$$

is the work done by the applied shear stress, and

$$\mathscr{S}_{\mathrm{TS}} = \int_0^{2\pi/\alpha} \left[-\frac{d^2\overline{u}}{dz^2}(1)\,\eta' u'\right]_{z=1} dx, \tag{6.2d}$$

is the work done by disturbance tangential stresses. Because of the particular form of the basic-state solution, i.e. $\overline{u}(z) = z$, we see that $\mathscr{S}_{\mathrm{TS}} = 0$. Thus, we shall disregard this term throughout the rest of the discussion. Each term in (6.1a) is computed using the eigenfunctions from linear theory.

To investigate the case of small surface tension, the terms in the energy balance were computed for $S = 0, \alpha = \alpha_c = 2{\cdot}43$, and for six values of R in the range [30, 1000], which includes the neutral point. Equation (6.1a) was satisfied by the calculated eigenfunctions to five significant figures near $R = R_c$, showing that the computations are self-consistent. Figure 11 shows each term in the energy equation over the given range of R. Just above $R = R_c$, the disturbances receive energy from the mean flow through Reynolds stresses and from stress working at the free surface. Because $S = 0$, the work done by surface-tension forces is identically zero. Thus, $\mathscr{S}$ is composed entirely of work done by the applied surface stress. All three terms on the right-hand side of (6.1a) decrease with increasing R, but the surface-stress-working term decreases faster than the Reynolds-stress term. As $R \to \infty$, $d\mathscr{E}/dt \to 0$, which is consistent with the inviscid stability of the liquid layer.

To investigate the case of large surface tension, the terms in the energy balance

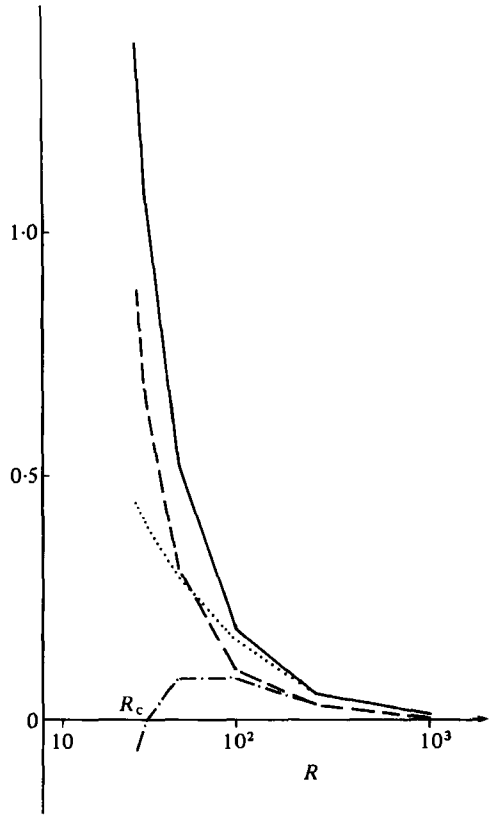

FIGURE 11. The terms in the energy equation (6.1*a*) for the linear velocity profile $\bar{u}$ for $S = 0$ and $\alpha = \alpha_c = 2{\cdot}43$. – · – · –, $d\mathscr{E}/dt$; . . . . . , $\mathscr{P}$; – – –, $R^{-1}\mathscr{S}$; ——, $R^{-1}\mathscr{D}$. The vertical scale is relative because of the arbitrary normalization of the eigenfunctions from linear theory. Computed points are connected by straight lines.

were computed for $S = 10^4$, $\alpha = \alpha_c = 1{\cdot}85$, and for nine values of R in the range [330, 5020], which includes the neutral point. Here, (6.1*a*) was satisfied by the computed eigenfunctions to four significant figures near $R = R_c$. Figure 12 shows that Reynolds-stress production is the major supplier of energy to the disturbances and that it actually increases as R moves through R_c. As with the $S = 0$ case, the dissipation and the work of the applied surface stress smoothly decrease with R. However, the work of surface-tension forces is positive for $R < R_c$, zero when $R = R_c$, becomes negative for $R > R_c$, decreases to a minimum at $R = 501$, and then increases to zero faster than any other term. Note that the work of surface-tension forces on the disturbances is the negative of the work required to change the surface area of the free surface. For $R < R_c$, the layer is stable and decays from its initial disturbance to zero. The free surface decreases its surface area during the decay, thereby feeding the energy stored during the initial deflection to the velocity disturbances; thus $\mathscr{S}_{ST} > 0$. At $R = R_c$, the disturbance is neutrally stable, and the free surface neither increases nor decreases its surface area; so $\mathscr{S}_{ST} = 0$. For $R > R_c$, the layer is unstable and the deflection of the free surface grows, thereby increasing its surface area. The energy for this increase in area comes from the disturbances; thus $\mathscr{S}_{ST} < 0$. As R is increased

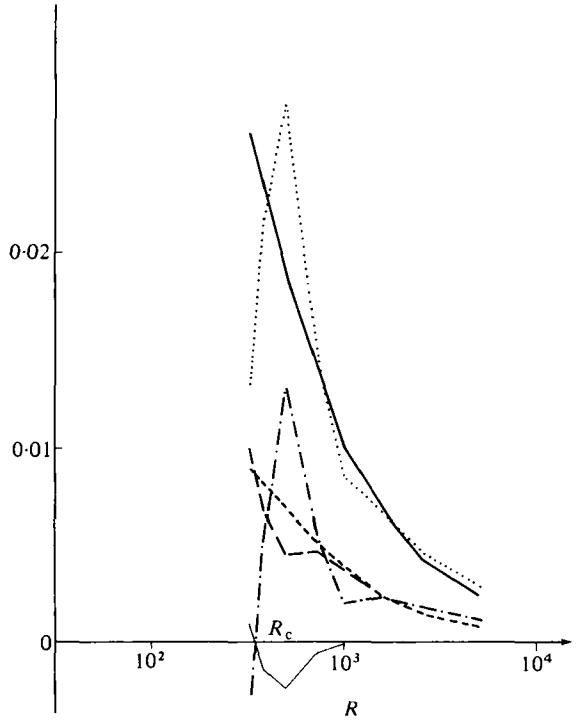

FIGURE 12. The terms in the energy equation (6.1a) for the linear velocity profile $\bar{u}$ for $S = 10^4$ and $\alpha = \alpha_c = 1{\cdot}85$. $-\cdot-\cdot-$, $d\mathscr{E}/dt$; ....., $\mathscr{P}$; — — —, $R^{-1}\mathscr{S}$; ——, $R^{-1}\mathscr{S}_{ST}$; - - - -, $R^{-1}\mathscr{S}_{NBS}$, ——, $R^{-1}\mathscr{D}$. The vertical scale is relative because of the arbitrary normalization of the eigenfunctions from linear theory. Computed points are connected by straight lines.

further, $\mathscr{S}_{ST}/R$ reaches a minimum and then goes to zero like R^{-2}, whereas $\mathscr{S}_{NBS}/R$ goes to zero only like R^{-1}.

For small surface tension, the layer becomes unstable because the rate of decrease of the Reynolds-stress production with R is slower than the rate of decrease of dissipation or surface stress working. However, energy for the instability is provided through work done by the applied stress and through Reynold-stress production. At larger values of surface tension the increase in Reynolds-stress production is the dominant mechanism for instability, while the surface stress working is of smaller importance. However, the presence of the free surface is vitally important to the overall instability of the system, for without it the system represents plane Couette flow in a channel, in which case the layer is always stable. In fact, as $S \to \infty$, the free surface becomes planar and stress-free and figure 4 shows that $R_c \to \infty$ as well; thus the layer would always be stable.

7. Parabolic velocity profiles and long-wave instabilities

Free-surface flows can sometimes exhibit a long-wave instability at low Reynolds numbers, as shown by Benjamin (1957) and Yih (1963) for film flow down an inclined plane. We shall investigate the long-wave instability of parallel shear flows driven by applied shear stresses; such flows in slots with end walls have parabolic velocity profiles.

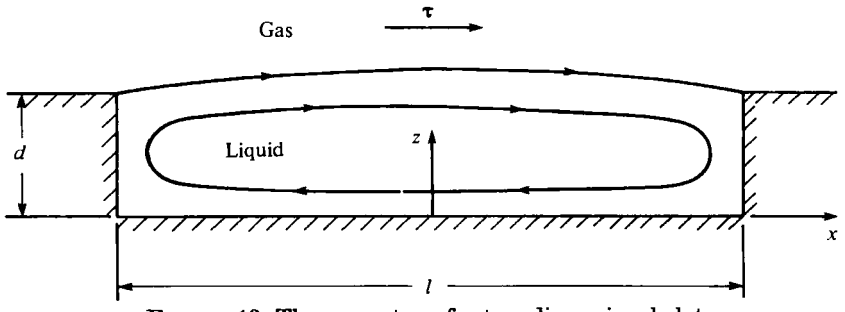

FIGURE 13. The geometry of a two-dimensional slot.

Liquid fills a two-dimensional slot as shown in figure 13. This slot has depth d and length l, and its aspect ratio is defined as

$$A \equiv d/l. \tag{7.1}$$

The flow field, driven by a constant shear stress on the interface, can be approximated asymptotically as $A \to 0$. In this case, there is at leading order a core region away from the ends composed of a parallel flow with zero mass flux through any vertical plane; the fluid turns around in end regions of dimension $O(A)$. The solutions in the two regions are connected through asymptotic matching. This method of solution is carried out in detail for a thermocapillary shear flow in a thin two-dimensional slot by Sen & Davis (1982). For the present case we find that the leading-order approximation of the flow field in the core region is given by

$$\overline{u} = \tfrac{3}{4}z^2 - \tfrac{1}{2}z + O(A), \tag{7.2a}$$

$$\overline{w} = 0 + O(A), \tag{7.2b}$$

$$\overline{\eta} = 1 + O(A), \tag{7.2c}$$

$$\overline{p} = \tfrac{3}{2}x + O(A). \tag{7.2d}$$

As discussed by Sen & Davis (1982) the approximation (7.2) is valid if $S \geqslant O(A^{-4})$. The stability of this leading-order approximation of the basic state can be found by employing the same linear stability analysis used in §2.3. We obtain for this leading-order approximation the Orr–Sommerfeld system (2.13), with

$$\overline{u} = \tfrac{3}{4}z^2 - \tfrac{1}{2}z. \tag{7.3}$$

We consider a long-wavelength disturbance to a flow with the velocity profile

$$\overline{u} = \overline{u}'(1)\,z + \tfrac{1}{2}\overline{u}''(1)\,(z^2 - 2z). \tag{7.4}$$

When $\overline{u}'(1) = 1$ and $\overline{u}''(1) = 0$, we have the linear velocity profile discussed previously. When $\overline{u}'(1) = 1$ and $\overline{u}''(1) = \frac{3}{2}$, we have the velocity profile for the core flow in a thin two-dimensional slot. We use regular perturbation theory for $\alpha \to 0$, $R = O(1)$, on the system (2.13), and obtain the complex phase speed

$$c = c_0 + i\alpha[\beta R - \tfrac{1}{3}\tilde{S}R^{-1}] + O(\alpha^2), \tag{7.5a}$$

where

$$c_0 = \overline{u}'(1) - \overline{u}''(1), \tag{7.5b}$$

$$\beta = -\tfrac{2}{15}c_0\overline{u}''(1), \tag{7.5c}$$

$$\tilde{S} = \alpha^2 S = O(1). \tag{7.5d}$$

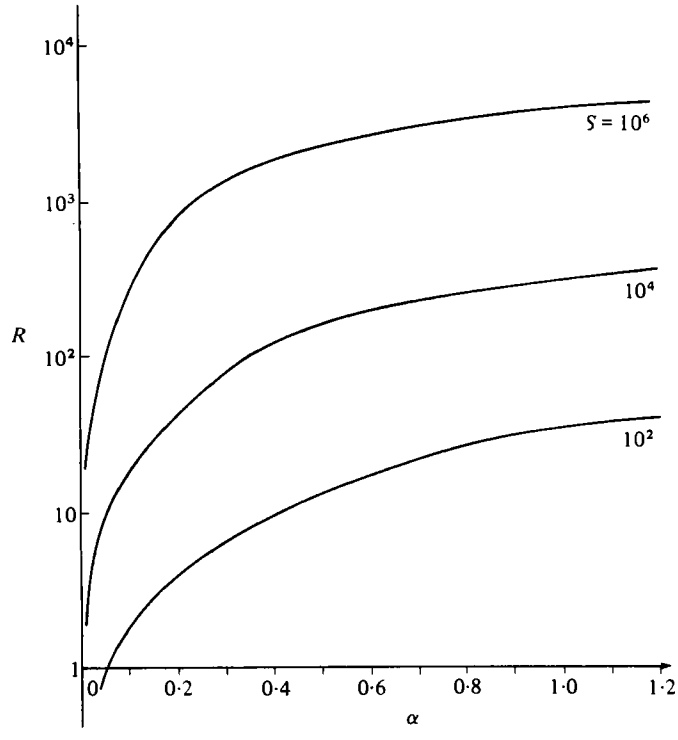

FIGURE 14. The computed neutral curves for the parabolic core-flow velocity profile $\bar{u}$ for various values of S.

When $\beta \leqslant 0$, the system is stable to long waves. When $\beta > 0$, the system is unstable to long waves, and the critical Reynolds number is given by

$$R_c = (\tilde{S}/3\beta)^{\frac{1}{2}}, \quad \alpha \to 0. \tag{7.6}$$

For the linear velocity profile, $\bar{u}'(1) = 1$ and $\bar{u}''(1) = 0$, and we have

$$c_0 = 1, \quad \beta = 0. \tag{7.7}$$

This velocity profile is, therefore, stable to long waves, consistent with our numerical calculations.

For the parabolic core-flow velocity profile $\bar{u}'(1) = 1$ and $\bar{u}''(1) = \frac{3}{2}$, and we have

$$c_0 = -\tfrac{1}{2}, \quad \beta = \tfrac{1}{10}. \tag{7.8}$$

Therefore we have a long-wave instability for this velocity profile, with the neutral curve given by

$$R_c = (\tfrac{10}{3}\tilde{S})^{\frac{1}{2}}, \quad \alpha \to 0. \tag{7.9}$$

Figure 14 shows numerically computed results for three values of S $(= \alpha^{-2}\tilde{S})$. For small α and $\tilde{S} = O(1)$ the computed curves agree with (7.9) to $O(\alpha^2)$ accuracy.

The difference between the long-wave instability results for the linear velocity profile and the parabolic core-flow velocity profile is easily traced to the change in sign of the parameter β. From the definition of β in (7.5c) and the observation that $\bar{u}'' = \bar{p}_x$ we can say the following about liquid layers with constant curvature velocity profiles:

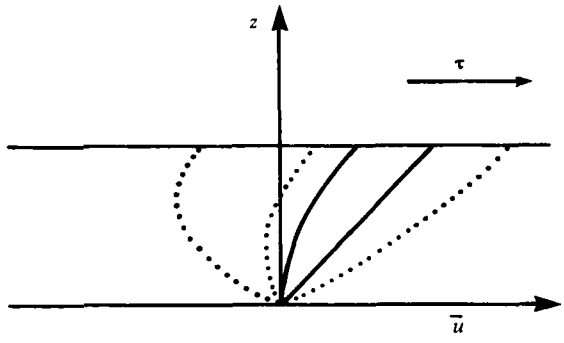

FIGURE 15. A sketch of the result (7.10) for constant-curvature velocity profiles normalized by setting $\bar{u}'(1) = 1$. Stable velocity profiles are bounded by the two solid profiles. The dotted velocity profiles are unstable.

(i) the layer will be unstable to long waves if

$$\frac{\bar{u}'(1)}{\bar{u}''(1)} < 1; \tag{7.10}$$

(ii) unstable long-wavelength disturbances to the layer always travel in the direction of decreasing pressure;

(iii) the phase speed of unstable long-wavelength disturbances is not contained in the range of $\bar{u}$.

The result (7.10) is sketched in figure 15 for velocity profiles normalized by setting $\bar{u}''(1) = 1$. Only those profiles bounded by the two solid ones are stable. It is interesting to note that any velocity profile with a region of return flow will be unstable to long waves.

Given a parabolic velocity profile of the basic state, one might expect a viscous instability similar to that in plane Poiseuille flow. For the velocity profile $\bar{u} = \frac{3}{4}(z^2 - 2z)$ and a redefinition† of the parameter S in the Orr–Sommerfeld system (2.13), we obtain the system which governs the instability of flow down an inclined plane. As De Bruin (1974) has shown, this problem does have a viscous instability at large Reynolds numbers. By superimposing a linear velocity profile on this parabolic one we regain the core-flow velocity profile (7.3). Potter (1966) shows that such a super-position is stabilizing for the case of Poiseuille flow in a *rigid channel*, and that when the maximum velocity of the linear component exceeds 0·7 times the maximum velocity of the plane Poiseuille component, the flow is always linearly stable. Our calculations also show a stabilizing trend when the plane Couette component increases, and we find no viscous instability for the core-flow velocity profile (7.3).

8. Discussion and conclusions

The term in the disturbance normal-stress boundary condition (2.9*e*) omitted by Miles (1960) accounts for a reduction of R_c by about a factor of two when $S = 0$. This reduction can be explained by examining the surface-stress-working term of the mechanical-energy balance. As shown in figure 11, when the liquid layer becomes

† Here $S = 2R\alpha^{-2}\cot\beta_0$, where β_0 is the angle of inclination of the rigid plane.

unstable for $S = 0$ the disturbances receive more than half of their energy from work done by the applied surface stress. No work is done by surface-tension forces, since $S = 0$. In omitting this surface-stress term Miles omits this source of energy.

If gravity were included in the present model, the only change in the disturbance equations would be the addition of the term $(-GR^{-1}\eta')N_i$ on the right-hand side of the normal-stress boundary condition (2.9*e*), where

$$G = gd^3\rho^2/\mu^2 \tag{8.1}$$

and g is the acceleration of gravity. This corresponds to replacing S by $S + G\alpha^{-2}$ in the boundary condition (2.13*e*).

In typical experiments (e.g. Craik 1966; Saric & Marshall 1971) the velocity profile is linear, and long-wave instabilities are absent. The depth of the layer is at most about 0·1 cm. While the corresponding value of G may be appreciable, the effect of gravity is usually small compared with the surface tension as measured by the Bond number $B_0 = GS^{-1} = \rho g d^2/\sigma$. By making the substitution $S + G\alpha^{-2} \rightarrow S$, it is seen that gravity can be neglected altogether when $B_0\alpha^{-2} \ll 1$. For example, in a 0·1 cm layer of water $S = 72800, G = 9800$ and $B_0 = 0{\cdot}13$. From figure 5, $\alpha_c = 1{\cdot}82$ and so $B_0\alpha_c^{-2} = 0{\cdot}041 \ll 1$. The addition of gravity changes the critical Reynolds number from 780 to 800, a change of less than 3%. As d decreases, B_0 will decrease, S will decrease causing α_c to increase, and so $B_0\alpha_c^{-2}$ will always be much less than unity. Thus it is reasonable to neglect gravity altogether. Note that this neglect always underestimates the critical Reynolds number. However, if the velocity profile were parabolic and long-wave instabilities were possible, then the quantity $G\alpha^{-2}$ would not necessarily be small and hence gravity might be important.

The problem actually solved by Miles models the upper fluid as only producing the mean shear flow in the layer, and ignores any other forces exerted by the gas on the liquid. Thus he ignores any direct energy transfer from the gas to the disturbances in the liquid. The problem solved in the present paper includes the normal-stress perturbation exerted by the gas on the liquid that is needed to keep the basic state shear stress exerted by the gas parallel to the surface of the liquid. As we have shown, this additional force lowers the critical Reynolds number significantly at small values of the parameter S.

A more general model assumes that the gas exerts both normal and tangential stress perturbations on the liquid as a result of surface deformation. Cohen & Hanratty (1965) use such a model in their analysis of wave formation on liquid layers. They use the work of Benjamin (1959) and Miles (1962) to determine the additional stress perturbations of the gas on the liquid and also include the surface-stress term in the normal-stress boundary condition that was omitted by Miles (1960). When the additional stress perturbations of the gas on the liquid are zero, their Orr–Sommerfeld system reduces to the system (2.13). While their large-Reynolds-number asymptotic analysis is in good agreement with their experimental observations, both show that the phase speed of the disturbances is larger than the interfacial velocity. They then conclude that the instability is a result of energy transfer from the gas to the liquid through the normal and tangential stress perturbations of the gas on the liquid. The appearance of slow waves, i.e. disturbances whose phase speeds are less than the interfacial velocity consistent with the present work, are not observed.

Craik (1966), however, does observe slow waves at very large wavelengths and small

Test number	S	R_{SM}	R_c
5	4310	120	255
6	4030	140	250
7	5470	195	275
17	4650	120	261
18	4620	136	261
19	5240	179	270
20	6860	260	300
22	5110	225	270
26	3070	100	228

TABLE 1. A comparison of the experiments of Saric & Marshall (1971) with the results of our linear stability theory. The test number and R_{SM} are from table 3 of Saric & Marshall (1971). The parameter S was calculated from their table 3 using the relation $S = R^2/W$. Using this value of S, R_c was obtained from our figure 4. For each test, Saric & Marshall (1971) report that the wavenumber and phase speed of the disturbance are approximately 0·1 and 0·7 respectively. Our calculations show that the wavenumber and phase speed should be 1·84 and 0·34 respectively.

Reynolds numbers. In his analysis, he uses the results of Benjamin's (1959) analysis of flow over a rigid wavy boundary for the normal and tangential stress perturbations of the gas on the liquid. He then follows the method used by Benjamin (1957) to obtain his long-wave instability criterion. As with Cohen & Hanratty (1965), Craik's long-wave instability receives its energy from the external forces applied on the free surface of the liquid by the bounding gas. Without these additional forces the layer is always stable to long waves as we have seen.

In the experiments of Saric & Marshall (1971) on supersonic flow over thin liquid layers, slow waves are observed at large Reynolds numbers. It is conjectured that the parallel-flow instability mechanism studied by Miles (1960) could possibly explain the existence of these waves. Table 1 compares their results for slow waves with the calculations presented in figures 4, 5 and 6. The experimental flows are unstable at values of the Reynolds number considerably below those predicted by our linear theory. In addition, the wavenumbers are an order of magnitude smaller and the phase speeds are twice as large as predicted. In any such experiment there will always be competing instability mechanisms present owing to the stress perturbations of the gas flow on the liquid interface. Because of this competition, and the possibility of nonlinear interactions between the various modes, the observed value of R_c can be altered significantly. Thus the difference between the experimental values of R_c and our linear theory might not be significant. Furthermore, because of errors involved in the calculation of the interfacial velocity and the effects mentioned above, the difference in the phase speeds may not be significant either. However, the large difference between the wavenumbers does suggest that the slow waves observed by Saric & Marshall (1971) are not the result of the parallel-flow mechanism studied by Miles (1960).

It is noted by Saric & Marshall (1971) for $R > 100$ that there is a definite observable change in the behaviour of the interface. Also observed, but not reported, was the existence of a very small scale structure superimposed on the long waves. This fine structure could not be measured at that time, but could be evidence of an instability with $\alpha \approx 2$, i.e. an instability caused by the parallel-flow mechanism. It was these qualitative observations that led to the conjecture of Saric & Marshall (1971) that the

parallel-flow mechanism was operating in these experiments. The validity of this conjecture can only be determined by further experiment.

The results obtained in this paper should properly be compared to an experiment in which the wave-induced stress perturbations of the gas on the liquid are negligible or zero. Such a situation would presumably arise in a thermocapillary shear flow. We have shown (Smith & Davis 1981) that for large values of the surface-tension number S the stability of an infinite two-dimensional thermocapillary shear flow to two-dimensional disturbances is governed by the stability characteristics of the problem considered in this paper. Furthermore, for a thermocapillary shear flow in the core region of a two-dimensional slot, we find that in the limit of small Prandtl and/or large surface Biot number the stability is also governed by the corresponding isothermal problem. However, experimental results for flows of this type are unavailable for comparison at this time.

The parabolic core flow in thin two-dimensional slots only exists away from the ends of the slot. The long-wavelength disturbances near $\alpha = 0$, found to be unstable in the core flow by the perturbation method, will be affected by the presence of the ends. One would expect that the ends would stabilize these long waves and that this effect would begin when the wavelength of the disturbance was comparable with the length of the slot. Thus the results of the long-wave analysis would have to be modified for end effects when

$$\alpha \leqslant 2\pi A. \tag{8.2}$$

However, the long-wave analysis is valid only for $\alpha < 2\pi A$. Only by extending the analytic results to larger α by numerical computation as shown in figure 14 can we describe instabilities that are negligibly affected by the presence of the end walls.

The authors wish to thank Prof. W. H. Reid for his advice on Orr–Sommerfeld asymptotic analysis and Prof. W. S. Saric for his advice and further information on the experiments of Saric and Marshall. This work was supported through contract no. NAS8-33881, National Aeronautics and Space Administration; Materials-Processing-in-Space-Program. M.K.S. is grateful for support under an IBM Fellowship.

REFERENCES

BENJAMIN, T. B. 1957 *J. Fluid Mech.* **2**, 554.

BENJAMIN, T. B. 1959 *J. Fluid Mech.* **6**, 161.

COHEN, L. S. & HANRATTY, T. J. 1965 *A.I.Ch.E. J.* **11**, 138.

CRAIK, A. D. D. 1966 *J. Fluid Mech.* **26**, 369.

DE BRUIN, G. J. 1974 *J. Engng Math.* **8**, 259.

FELDMAN, S. 1957 *J. Fluid Mech.* **2**, 343.

HOWARD, L. N. 1961 *J. Fluid Mech.* **10**, 509.

MILES, J. W. 1960 *J. Fluid Mech.* **8**, 593.

MILES, J. W. 1962 *J. Fluid Mech.* **13**, 433.

POTTER, M. C. 1966 *J. Fluid Mech.* **24**, 609.

SARIC, W. S. & MARSHALL, B. W. 1971 *A.I.A.A. J.* **9**, 1546.

SCOTT, M. R. & WATTS, H. A. 1975 *Sandia Labs, Albuquerque, Rep.* SAND75-0198.

SCOTT, M. R. & WATTS, H. A. 1977 *SIAM J. Numer. Anal.* **14**, 40.

SEN, A. K. & DAVIS, S. H. 1982 *J. Fluid Mech.* **121**, 163.

SMITH, M. K. & DAVIS, S. H. 1981 *European Mechanics Colloquium* 138, *University of Karlsruhe, March* 1981.

YIH, C. S. 1963 *Phys. Fluids* **6**, 321.